

Micelle formation of randomly grafted copolymers in slightly selective solvents

Adam Kreig

Department of Chemical Engineering, Chemistry and Materials Science, Polytechnic University, Brooklyn, New York 11201

Amy A. Lefebvre, Hyeok Hahn, and Nitash P. Balsara

Department of Chemical Engineering and Materials Science Division, Lawrence Berkeley National Laboratory, University of California, Berkeley, California 94720

Shuyan Qi

Department of Chemical Engineering, University of California, Berkeley, California 94720

Arup K. Chakraborty

Department of Chemical Engineering, Department of Chemistry, and Materials Science Division, Lawrence Berkeley National Laboratory, University of California, Berkeley, California 94720

Maria Xenidou and Nikos Hadjichristidis

Department of Chemistry, University of Athens, Panepistiomiopolis Zografou 15771, Athens, Greece

(Received 15 December 2000; accepted 27 June 2001)

Amphiphilic surfactants, molecules with chemical moieties that interact differently with the solvating medium, are important for technological applications and ubiquitous in biology. Understanding how to control surfactant properties is, therefore, of wide-ranging importance. Using a combination of light scattering experiments and field theory, we demonstrate that the behavior of polymeric surfactants can be controlled sensitively by manipulating molecular architecture. We find that branched polymeric amphiphiles can be much better surfactants than traditional linear analogs. This is indicated by micelle formation in solvents that are very slightly selective for the backbone of the branched molecule. Our experimental and theoretical findings also suggest that, for a given chemistry and architectural class, surfactant properties of polymeric amphiphiles are very sensitive to subtle changes in architectural features. Specifically, we find that choosing a particular branching density optimizes the propensity for micelle formation. The sensitivity of macromolecular surfactant properties to molecular architecture can perhaps be profitably exploited in applications wherein only certain chemical moieties are allowed. The physical origin of this sensitivity is the importance of conformational entropy penalties associated with the pertinent self-assembly process. This is in contrast to self-assembly of small molecule systems where conformational entropy is not of such significance. © 2001 American Institute of Physics. [DOI: 10.1063/1.1395559]

I. INTRODUCTION

The ability of amphiphilic molecules to form organized assemblies in solution has important commercial and biological consequences.^{1,2} A variety of products such as detergents, emulsifiers, catalysts, and vesicles for drug delivery rely on this ability. Membranes in plant and animal cells are composed of self-assembled phospholipid bilayers. Self-assembly into these organized motifs is driven by the amphiphilic character of the molecular building blocks (i.e., different chemical groups in the molecules exhibit different solvent affinities). The simplest organized assembly is a micelle, which is formed to minimize unfavorable interactions between the medium and the poorly solvated moieties of the amphiphile. Although a large majority of studies have been conducted using water as the solvent, the amphiphilic character of molecules can be expressed in a variety of media such as organic solvents and polymers.¹⁻⁴ Extensive theoretical and experimental studies of micelles formed by single-

tailed and double-tailed amphiphiles [Fig. 1(a)], including those of biological importance, have been conducted (e.g., Refs. 1-7). Recent studies have focused on synthetic double-tailed surfactants (Gemini surfactants) due to their superior properties (e.g., Ref. 8). However, most efforts to control surfactant properties focus on the proper choice of the chemical structure of the amphiphilic molecule.

This paper concerns macromolecular amphiphiles synthesized by connecting chemically dissimilar polymer chains [Figs. 1(b) and 1(c)]. We demonstrate that the surfactant properties of macromolecules (and hence their ability to self-assemble into functionally interesting motifs) can be controlled with high sensitivity by manipulating molecular architecture without changing the chemical identity of the amphiphilic moieties. In addition to differences in surfactant properties between macromolecules in different architectural classes, our findings show that subtle variations within an architectural class also lead to significant effects. This is due to the importance of conformational entropy for self-

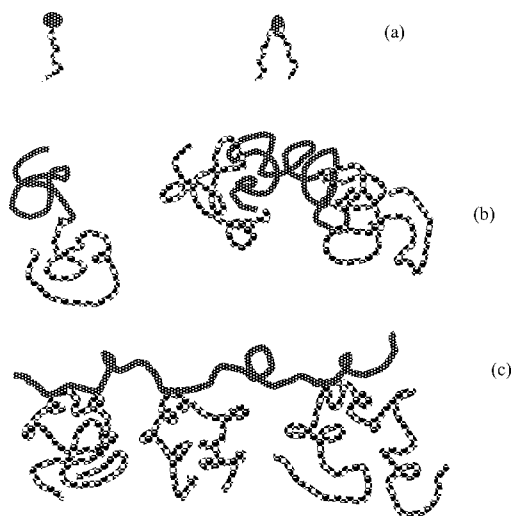


FIG. 1. Amphiphilic molecules. (a) Small molecule amphiphiles: single-tailed and double-tailed surfactants. (b) Linear polymeric amphiphiles: diblock and triblock copolymers. (c) Branched amphiphiles with a well-solvated backbone and poorly solvated branches.

assembly processes of polymers. This notion of choosing the nature of the connections between the amphiphilic moieties to control surfactant properties may prove useful in applications where the choice of chemical structure is restricted (e.g., for concerns related to biocompatibility or toxicity).

We use light scattering experiments and a field-theoretic model to show that randomly grafted copolymers [see Fig. 1(c)] are extremely efficient surfactants. It is worth remarking that *agrecans*, one of the most effective biological surfactants, have a similar architecture.⁹ We find that, for the branched macromolecules shown in Fig. 1(c), a slight affinity of the medium toward the backbone relative to the branches is sufficient for micelle formation. Such a small selectivity is insufficient to induce micelle formation in linearly connected polymeric amphiphiles such as diblock copolymers [Fig. 1(b)]. In addition, we show that an intermediate branching density optimizes surfactant properties due to the interplay between molecular architecture and conformational entropy.

II. EXPERIMENTS

Polybutadien-polystyrene (PB-PS) branched copolymers were synthesized by a combination of anionic polymerization and silane coupling.¹⁰ The resulting polymer consists of a PB backbone with randomly located tetrafunctional graft points. The middle of the polystyrene chains is grafted on to the backbone, as shown in Fig. 1(c). The backbone, the grafts, and the graft copolymers were characterized by size exclusion chromatography, light scattering, and NMR spectroscopy measurements. The characterization results are summarized in Table I. The principal difference between the two copolymers is the average number of grafts per molecule (P). The copolymers are labeled BC-10 and BC-18, where the number indicates P . The same backbone was used to synthesize both polymers, and the graft molecular weights are approximately 20 kg/mol in both cases.

TABLE I. Characteristics of the branched copolymers.

Sample	Molecular weight of PB backbone (kg/mol)	Molecular weight of PS branch (kg/mol)	Average number of branches per molecule	Total molecular weight (kg/mol)
BC-10	100	19	10	390
BC-18	100	23	18	610

Dynamic light scattering (DLS) data from toluene solutions of BC-10 and BC-18 were acquired on an ALV-5000 instrument.¹¹ Solutions ranging from 1.0 to 2.5 wt. % polymer were examined. Samples were prepared by filtering HPLC grade toluene (Aldrich) from freshly opened bottles into glass cuvettes that contained the appropriate amount of the copolymer. The cuvettes containing the polymer solutions were flame sealed, annealed at 70 °C for about 1 h, and cooled slowly (over a period of 6 h) to room temperature. The light scattering data obtained from the annealed copolymer solutions during heating and cooling runs were identical.

A Nd:YAG solid-state laser (wavelength $\lambda = 0.532 \mu\text{m}$) was used as the source and scattering data were obtained at several scattering angles θ between 30° and 150°. The time autocorrelation function of the scattering light intensity, $g(\tau)$, was measured in the homodyne mode. In dilute solutions, $g(\tau)$ is related to the mobility of the scattering entities. In Fig. 2(a) we show $g(\tau)$ measured from a 1.5 wt. % solu-

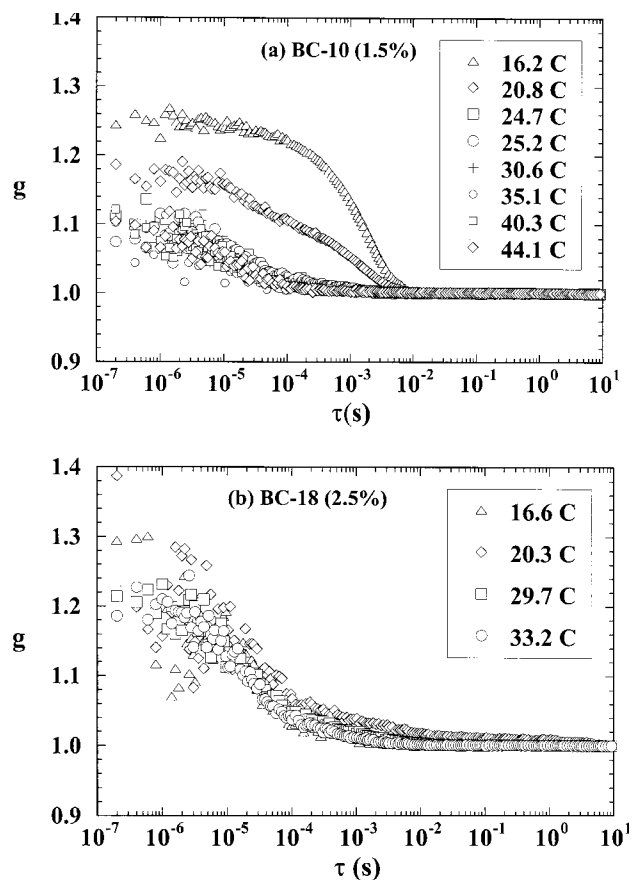


FIG. 2. Autocorrelation function of the scattered light, $g(\tau)$, at selected temperatures (a) BC-10 solutions, (b) BC-18 solutions.

tion of BC-10 at selected temperatures for $\theta=90^\circ$. At temperatures (T) $\geq 24.7^\circ\text{C}$, the characteristic time for the decay of the autocorrelation function to the base line [where $g(\tau) = 1$] is in the vicinity of 10^{-5} s. This time scale is consistent with the diffusion time scales of individual BC-10 molecules in toluene. At 20.8 and 16.2 $^\circ\text{C}$, the characteristic time for the decay of the autocorrelation function is significantly larger than that obtained at high temperatures [see Fig. 2(b)]. The characteristic decay time at 16.2 $^\circ\text{C}$ is 2 orders of magnitude longer than that obtained at 24.7 $^\circ\text{C}$. This is a classic signature of intermolecular aggregation or micelle formation. The critical temperature for micelle formation in the 1.5% BC-10 solution is $23 \pm 2^\circ\text{C}$. The qualitative features of DLS data obtained from 2.0% and 2.5% BC-10 solutions were similar to the 1.5% solution data shown in Fig. 2(a). The formation of micelles was detected at temperatures below a threshold value.

Typical DLS data obtained from BC-18 solutions are shown in Fig. 2(b), where we have chosen to display data obtained from the 2.5% solution. We find characteristic decay times of 10^{-5} s over the entire experimental temperature window. We thus see no evidence of micelle formation in BC-18 solutions.

The intensity-weighted distributions of mobilities, $G(\tau)$ were obtained by solving the following integral equation:

$$g(t) = B \left[a \left(\int_0^\infty d\left(\frac{1}{\tau}\right) G(\tau) \exp(-t/\tau) \right)^2 + 1 \right] \quad (1)$$

using CONTIN.¹² The location of the peaks in the distribution function, $G(\tau)$, allow calculation of diffusion coefficients of the species in solution, $D = 1/(\tau_c k^2)$, where τ_c is the characteristic decay time of the species and $k = 4\pi \sin(\theta/2)/\lambda$. The hydrodynamic size of the species, R_h was then estimated from the Stokes–Einstein relationship,

$$D = \frac{k_B T}{6\pi\eta R_h}, \quad (2)$$

where k_B is the Boltzmann constant, T is the absolute temperature, and η is the solvent viscosity. All of the BC-18 solutions exhibited a single τ_c corresponding to R_h values between $0.003\mu\text{m}$ and $0.004\mu\text{m}$. These values are comparable to R_h values of PS and PB homopolymers of similar molecular weights in toluene. We thus conclude that the BC-18 polymer is molecularly dispersed in toluene in the entire concentration and temperature window. We show the temperature dependence of R_h obtained from the 2.5% BC-18 solution in Fig. 3 (hatched squares). Also shown in Fig. 3 is the temperature dependence of R_h obtained from BC-10 solutions. The presence of aggregates with $R_h = 0.3\mu\text{m}$ is evident at lower temperatures (below 35 $^\circ\text{C}$) while free molecules are detected at high temperatures (above 35 $^\circ\text{C}$). In the temperature range between 24 and 35 $^\circ\text{C}$, the micelles and free chains are seen to coexist while at temperatures below 24 $^\circ\text{C}$ only micelles are detected.

The presence of aggregates was also studied by static light scattering (SLS) measurements conducted on the same samples, using the same ALV-5000 instrument. In Fig. 4(a) we show the k -dependence of the static scattering intensity,

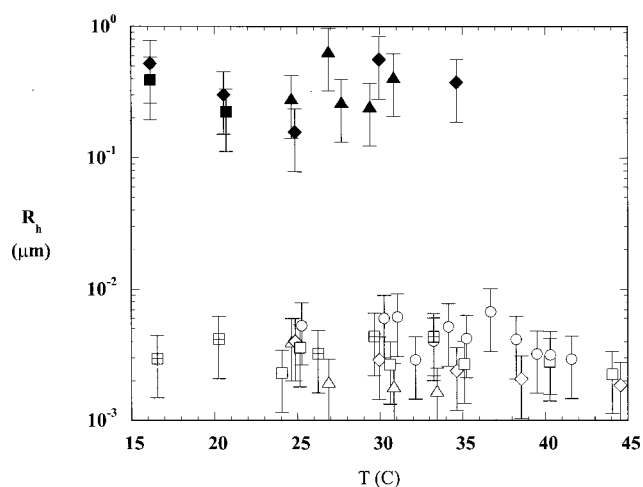


FIG. 3. Temperature dependence of the hydrodynamic radius in BC-10 and BC-18 solutions. Hatched squares, BC-18, 2.5%; circles, BC-10, 1.0%; squares, BC-10, 1.5%; diamonds, BC-10, 2.0%; triangles, BC-10, 2.5%. The hollow symbols represent the individual molecules while the solid symbols represent the micelles.

$I(k)$, for the 1.5% BC-10 solution. At high temperatures we see scattering intensities in the range of 10^{-4}cm^{-1} . At lower temperatures (20.3 and 16.6 $^\circ\text{C}$) we find intensities ranging from 10^{-3} to 10^{-2}cm^{-1} . In contrast, the $I(k)$ data from BC-18 solutions in the 10^{-4}cm^{-1} range at all concentrations and temperatures, are shown in Fig. 4(b). The SLS measurements confirm the presence of micelles in BC-10 solutions

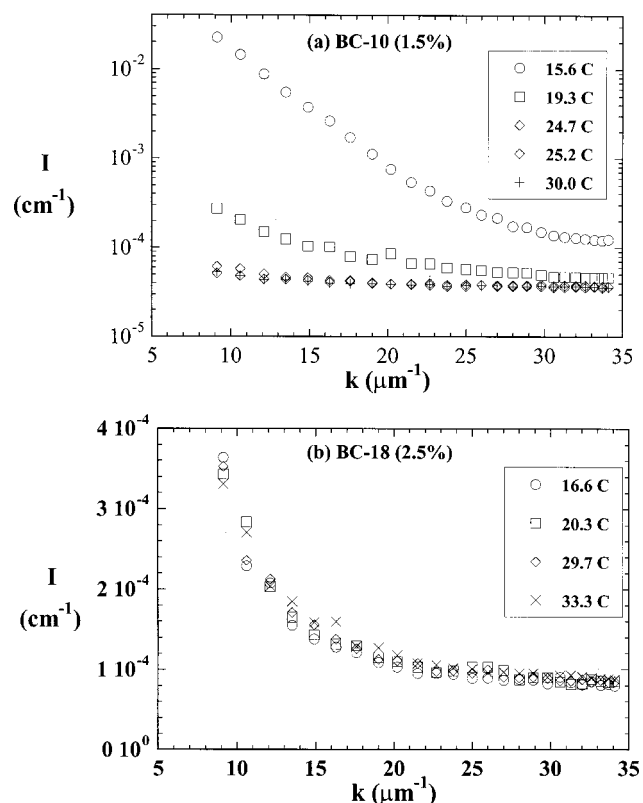


FIG. 4. Static light scattering profiles, $I(q)$, at selected temperatures (a) BC-10 solutions. (b) BC-18 solutions. Due to the large changes in $I(q)$ with temperature, the BC-10 data are shown on a log scale.

for $T < 20^\circ\text{C}$. At the lowest accessible k ($k = 8 \mu\text{m}^{-1}$), I increases by a factor of about 300 when the temperature is changed from 24.6°C (where the solution is composed of free chains) to 15.6°C (where the solution is composed of micelles). The average number of chains per micelle is given by the ratio I in the limit $k \rightarrow 0$. Such extrapolations can only be done with accuracy if $kR_g < 1$ (Zimm scattering). Using the measured value of $R_h \approx 0.5 \mu\text{m}$ (Fig. 3) as an approximate measure of R_g , we conclude that Zimm scattering would be observed in the $k < 2 \mu\text{m}^{-1}$ regime. It is thus clear that an accurate measure of the aggregation number of the micelles cannot be obtained from the data in Fig. 4. The factor of 300 that we have observed in the low k limit represents a lower limit for the aggregation number of the micelles. The large values of R_h and the steep dependence of static light scattering intensity from micelles on k [15.6 °C data in Fig. 4(a)] suggest that the micelles are nonspherical.

Most researchers (e.g., Refs. 13 and 14) consider toluene to be a common solvent for PB and PS chains. Micelle formation of branched PS-PB molecules in toluene is therefore surprising. Recent studies suggest that toluene is a slightly better solvent for polybutadiene than polystyrene.^{15–17} The micelles under consideration should thus consist of a core of polystyrene branches surrounded by a solvated corona predominantly made up of polybutadiene loops.

It is clear from the literature that PS-PB diblock copolymers do not form micelles in toluene.^{18,19} Thus, the first question we seek to answer is why do branched molecules form micelles in slightly selective solvents? In architecturally simple macromolecular amphiphiles, such as diblock copolymers, the tendency for micelle formation is enhanced by increasing molecular weight of the poorly solvated block.²⁰ Our observations show that this is not the case for branched macromolecules; BC-18 has a higher molecular weight compared to BC-10, but does not form micelles under conditions wherein the latter does. We now discuss a field-theoretic analysis and physical arguments that provide the underpinnings of our observations by addressing these issues, and show that molecular architecture is key for micelle formation in branched macromolecular surfactants.

III. THEORY

Consider a mixture of N_C randomly grafted copolymer chains (RGCs) and N_S solvent molecules. Generalizing ideas developed by us recently to study microphase ordering in molten RGCs,^{21,22} we can write down a theory which describes this situation. We first write down a microscopic Hamiltonian, which includes connectivity reflecting the polymer architecture, intersegment interactions, and segment-solvent interactions. The intersegment and segment-solvent interactions explicitly depend upon the chemical identity of the segments (i.e., whether they belong to a branch or to the backbone). This microscopic Hamiltonian is then rewritten in terms of the following macroscopic order parameter fields: $\rho_{\text{PS}}(\mathbf{r})$, $\rho_{\text{PB}}(\mathbf{r})$, and $\rho_S(\mathbf{r})$ which denote the densities of PS, PB, and solvent molecules, respectively. Each RGC chain in solution has a different sequence of branch point locations. A proper quenched average over the fluctuations in branch

point locations is performed using the replica method.²³ In so doing, we assume that the branch points are distributed with a mean value of P per chain and that the fluctuations in the positions of the branch points exhibit short-range correlations. These mathematical steps allow us to develop a Landau free energy functional up to quartic order. For our present purpose, we concern ourselves with the free energy functional up to quadratic order only. Detailed derivation of the free energy functional is provided in the Appendix. Here we simply write down the quadratic term of the free energy functional that we obtain. We denote it by F , and it is

$$\frac{F}{V} = \frac{1}{2} \int d\mathbf{q} \rho(\mathbf{q})^T \Gamma_2(\mathbf{q}) \rho(\mathbf{q}), \quad (3)$$

where $\rho(\mathbf{q})^T = (\rho_A(\mathbf{q}), \rho_B(\mathbf{q}), \rho_S(\mathbf{q}))$,

$$\Gamma_2(\mathbf{q}) = \begin{bmatrix} M_{AA}(q) & M_{AB}(q) & 0 \\ M_{BA}(q) & M_{BB}(q) & 0 \\ 0 & 0 & N_S \end{bmatrix}^{-1} + \begin{bmatrix} \chi_{AA} & \chi_{AB} & \chi_{AS} \\ \chi_{BA} & \chi_{BB} & \chi_{BS} \\ \chi_{SA} & \chi_{SB} & \chi_{SS} \end{bmatrix}, \quad (4)$$

and

$$\begin{aligned} M_{AA} &= N_C N^2 g_2 \left(\frac{Nq^2 b^2}{6} \right), \\ M_{AB} = M_{BA} &= N_C M N P g_1 \left(\frac{Mq^2 b^2}{6} \right) g_2 \left(\frac{Nq^2 b^2}{6} \right), \\ M_{BB} &= N_C \left[P M^2 g_2 \left(\frac{Mq^2 b^2}{6} \right) + M^2 P (P-1) \right. \\ &\quad \left. \times g_1^2 \left(\frac{Mq^2 b^2}{6} \right) g_2 \left(\frac{Nq^2 b^2}{6} \right) \right], \\ g_1(x) &= \frac{1 - \exp(-x)}{x}, \\ g_2(x) &= \frac{2}{x^2} [\exp(-x) + x - 1]. \end{aligned} \quad (5)$$

Here b is the statistical segment length (which we have taken to be the same for both PS and PB blocks for simplicity), M and N are the number of statistical segments in each branch and the backbone, respectively. In the equations above, A denotes the PB segments and B the PS segments. χ_{ij} denotes the Flory interaction parameter between the i - and j -type species. We note in passing that in the absence of the solvent, Γ_2 is a 2×2 matrix, which has been obtained before.^{21,24} As noted in these references, the matrix Γ_2 is different for randomly grafted copolymers compared to uniform comb polymers. The effect of this randomness is even more pronounced in the quartic terms of the free energy functional. Thus, we expect that CMC characteristics in a strong segregation limit theory, and the stability limit of the homogeneous phase to be strongly influenced by the quenched randomness embodied in the sequence of branch points. Some

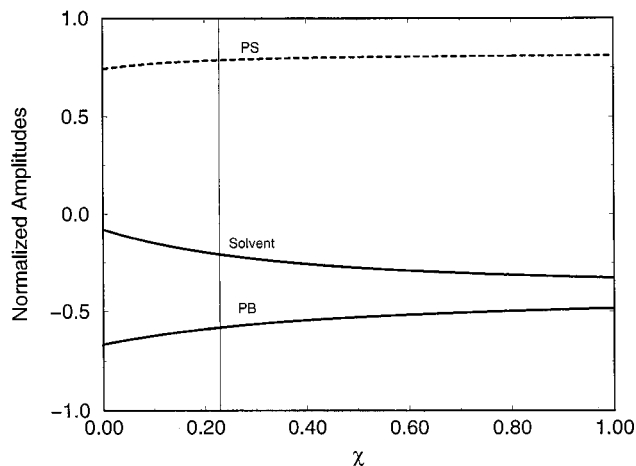


FIG. 5. The eigenvector which belongs to the smallest eigenvalue as a function of χ for $N=2138$, $M=285$, and $P=20$. The ordinate measures the amplitude of the concentration fluctuations of each species. The amplitudes are normalized by enforcing the sum of their squares to equal unity. The vertical line indicates the stability limit.

manifestations of these differences between random and uniform grafting for molten polymers have recently been described in Refs. 21, 24, 25.

This free energy functional can be employed to study the stability limit of the disordered state (free chains in solution with no segregation of the PS and PB blocks from each other or from the solvent), and the nature of the unstable concentration fluctuations at the point of instability. These concentration fluctuations are signatures of the state which results as the homogeneous state becomes unstable. The stability limit is obtained by finding the condition wherein Γ_2 is no longer positive definite. The eigenvector that belongs to the smallest eigenvalue of Γ_2 at the stability limit tells us the nature of the concentration fluctuations. We use Eqs. (3)–(5) to obtain the stability limit and pertinent eigenvectors.

In order to understand the qualitative behavior, we study the simplest model that contains the essential physics. Specifically, we take the solvent molecules to be chemically identical to the segments that constitute the backbone of the RGCs. (Due to this and other simplifications,²⁶ no quantitative inferences are to be drawn from the theoretical results.) We fix temperature, M , and N , and compute the concentration of RGC chains (C_{sl}) required for the disordered phase to become unstable. We compute C_{sl} as a function of P for various values of temperature. For all values of P and temperature, at the stability limit, we find that the eigenvectors associated with the unstable mode correspond to concentration fluctuations which are such that the solvent molecules and the backbone segments segregate from the segments that comprise the branches. This is illustrated in Fig. 5 for particular values of N , M , and P . Separation of backbone segments and solvent molecules from branch segments is a pathway that is necessary for micelle formation. Thus, these concentration fluctuations may announce the impending formation of micelles as the homogeneous state becomes unstable. Therefore, we may view C_{sl} to be directly related to the critical micelle concentration (but not equal to it).

Figure 6 shows that the variation of C_{sl} with P is non-

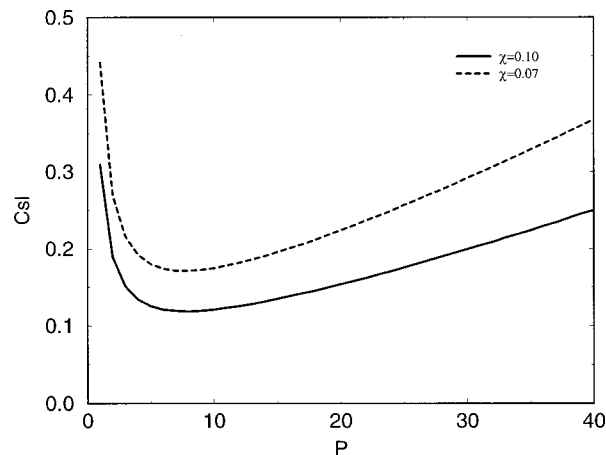


FIG. 6. Field-theoretic prediction of C_{sl} , the concentration at the stability limit, as a function of P for fixed values of N and M . Results are shown for two values of χ (i.e., temperature).

monotonic. When P is small it becomes easier to form micelles upon increasing the number of branches, and above an optimal value of P the opposite is true. Another feature of the results displayed in Fig. 6 is worth noting. As the solvent becomes less selective for the RGC's backbone, in the region where P is small, the magnitude of the slope of the curve that describes the variation of C_{sl} with P becomes larger.

The results displayed in Fig. 6 explain our experimental findings. It is harder to form micelles with BC-18 ($P=18$) compared to BC-10 ($P=10$) because these experiments appear to correspond to the regime wherein increasing P makes it harder to form micelles. The finding that it is easier to form micelles with RGCs (with the number of branches in a certain range) rather than their chemical analogs with simpler architectures is also made clear. Consider our theoretical predictions in the limit of $P=1$. This is a very simple architecture that is close to a linear system (diblock copolymer). As we see, it is much harder to form micelles in this case compared to several RGCs (i.e., those with larger values of P). This trend does not continue beyond a threshold value of P as indicated by both our theory and experiments. The non-monotonic dependence of C_{sl} on P also suggests that, for a given choice of monomers, we can obtain optimal surfactant properties of grafted copolymers by manipulating the branching density.

The physical reasons that underlie our experimental and theoretical findings are simple. As has been pointed out by many authors (e.g., Ref. 20), the equilibrium between a phase with micelles and free chains and the disordered phase with no micelles depends in an important way on the free energy per copolymer chain in a micelle. In our case, micelle formation is driven by the energetic advantage associated with protecting the branches from the solvent. Entropic penalties oppose micelle formation, and are different for polymers with different architectures. Simple geometric arguments allow us to understand our theoretical and experimental findings concerning the variation of surfactancy with polymer architecture in terms of these entropy penalties. Each micelle consists of a core made up of segments belonging to RGC branches and a solvated corona of

backbone segments. The architecture of RGCs necessitates that the PB segments that make up the corona be arranged such that the sections of PB segments between branch points form loops that return to the surface of the core made up of PS segments. The entropic penalties for micelle formation are associated with packing the core with branch segments and forming the loops that make up the corona. These entropy penalties depend upon the number of branches in different ways.

When P is small, the loops of polybutadiene that must form the corona are long (average length is N/P) and they need to protect a relatively small core. Loop entropy penalties are thus relatively small, and the entropic penalty for forming a micelle is dominated by that associated with packing the core. In this regime, increasing P reduces the entropic penalty for micelle formation. This is because as the number of branches increases the number of PS segments per copolymer chain increases, and it becomes easier to pack the core since each branch has to deform less. As P increases, the average loop length is smaller and the PB segments need to cover a larger area to protect the core (i.e., the average distance between loop ends is larger). The entropic penalty associated with arranging the polybutadiene loops becomes larger as P increases because the average loop length decreases and the average distance between loop ends grows. Beyond a threshold value of P , the entropic penalty for forming the micelle is dominated by that required to form the loops that make up the corona. Thus, in this regime, it becomes harder to form micelles as P increases. These simple arguments explain our main findings. A “strong segregation limit” theory^{20,27} may provide insight into the field-theoretic prediction that C_{sl} decreases more strongly with P (in the small P regime) as the solvent becomes less selective, and may also allow the development of scaling relationships which can guide the choice of architecture for obtaining desired surfactant properties. We hope to report on these issues in the future. Our results also indicate the need for more extensive experiments on a series of RGCs with different architectures (e.g., fixed M and N but varying P over a wide range) in slightly selective solvents. It is also necessary to explore the self-assembly of the RGCs as a function of solvent selectivity. This will provide a bridge between the present work and more traditional studies of the interfacial properties RGCs.^{28,29}

IV. CONCLUSION

Controlling the way in which molecular building blocks can self-assemble in solution is important for many applications. Our most significant finding is that manipulating molecular architecture is a sensitive way to tune surfactant properties of macromolecules. Unlike small molecules, the behavior of macromolecules is often dominated by conformational entropy contributions, and this makes molecular architecture a sensitive “knob” for controlling surfactant properties of polymers. Our specific findings (and future efforts) regarding micelle formation by RGCs may be of some significance to biology. The remarkable surfactancy of phospholipids, which are double-tailed in architecture, is well understood.⁶ There are however, a plethora of biological sur-

factants that are macromolecules with more than two branches (e.g., *agrecans*⁹) where the role of molecular architecture remains to be elucidated. We have found that branched copolymers are good model systems for studying the relationships between surfactancy and molecular architecture. Insight into these relationships should prove to be useful for applications.

ACKNOWLEDGMENTS

Financial support provided by the National Science Foundation (CTS-0196066, DMR-9901951), and U.S.D.O.E. (B.E.S) are gratefully acknowledged. A.K.C. and N.P.B. are Camille–Dreyfus Teacher–Scholars.

APPENDIX

The system we consider contains N_C RGC chains. Each chain has a backbone with N monomers of A-type, and P branches, each with M monomers of B-type. The number of solvent molecules is N_S . For this system, the partition function is

$$Z = \left\{ \prod_{i=1}^{N_C} \prod_{j=1}^P \prod_{m=1}^{N_S} \int D\mathbf{r}_i(n) D\mathbf{r}_{ij}(s) D\mathbf{r}_m \right. \\ \left. \times P_0[\mathbf{r}_i(n)] P_0[\mathbf{r}_{ij}(s)] \delta[\mathbf{r}_{ij}(0) - \mathbf{r}(\tau_{ij})] \right\} \exp[-E], \quad (\text{A1})$$

where we use $k_B T$ as a unit for energy (k_B is the Boltzmann constant, T is temperature). $\mathbf{r}_i(n)$, $\mathbf{r}_{ij}(s)$, and \mathbf{r}_m are the positions of the n th monomer on the backbone of the i th chain, the s th monomer on the j th branch of the i th chain, and the m th molecule of the solvent, respectively. $P_0[\mathbf{r}_i(n)]$ and $P_0[\mathbf{r}_{ij}(s)]$ ensure the connectivity of the backbones and the branches, i.e., explicitly,

$$P_0[\mathbf{r}_i(n)] = C_N \exp \left[-\frac{3}{2b^2} \int_0^N dn \left(\frac{\partial \mathbf{r}_i(n)}{\partial n} \right)^2 \right], \\ P_0[\mathbf{r}_{ij}(s)] = C_M \exp \left[-\frac{3}{2b^2} \int_0^M ds \left(\frac{\partial \mathbf{r}_{ij}(s)}{\partial s} \right)^2 \right], \quad (\text{A2})$$

where C_N and C_M are normalization constants, and b is the statistical segment length for both monomer A and B. The δ -function in Eq. (A1) ensures the connectivity of the branches to specific points on the backbone. τ_{ij} are the positions of the branch points ($j=1$ to P) on the backbone of the i th chain. The distribution of τ_{ij} is random, and we shall perform a quenched average over this distribution.²³ Let us introduce coarse-grained macroscopic densities of different species, $\rho_A(\mathbf{r}) = \sum_{i=1}^{N_C} \int dn \delta[\mathbf{r} - \mathbf{r}_i(n)]$, $\rho_B(\mathbf{r}) = \sum_{i=1}^{N_C} \sum_{j=1}^P \int ds \delta[\mathbf{r} - \mathbf{r}_{ij}(s)]$, and $\rho_S(\mathbf{r}) = \sum_{m=1}^{N_S} \delta[\mathbf{r} - \mathbf{r}_m]$. We also define the volume to be $V = N_C(N + PM) + N_S$ so that the total density of all species equals 1 (phenomenology of a lattice model). $E = E(\rho_A, \rho_B, \rho_S)$ is the interaction energy, and it has the form

$$E = \frac{V}{2} \int d\mathbf{r} \boldsymbol{\rho}(\mathbf{r})^T D \boldsymbol{\rho}(\mathbf{r}), \quad (\text{A3})$$

where $D_{ij} = \chi_{ij}$ are Flory interaction parameters between the i - and j -type species. $\boldsymbol{\rho}^T = (\rho_A, \rho_B, \rho_S)$. We now define the entropy to be

$$S = \ln(R) = \ln \left\{ \prod_{i=1}^{N_C} \prod_{j=1}^P \prod_{m=1}^{N_S} \int D\mathbf{r}_i(n) D\mathbf{r}_{ij}(s) D\mathbf{r}_m \right. \\ \left. \times P_0[\mathbf{r}_i(n)] P_0[\mathbf{r}_{ij}(s)] \delta[\mathbf{r}_{ij}(0) - \mathbf{r}(\tau_{ij})] \right\}, \quad (\text{A4})$$

such that $Z = \exp[S - E]$. Thus, the quenched average need be performed on the entropy only, and we use the replica trick to compute this average,

$$\langle S \rangle = \lim_{\sigma \rightarrow 0} \frac{\langle R^\sigma \rangle - 1}{\sigma}. \quad (\text{A5})$$

Here the average is taken over the quenched distribution of τ_{ij} . These considerations lead to

$$\langle R^\sigma \rangle = \left\langle \prod_{\alpha=1}^\sigma \prod_{i=1}^{N_C} \prod_{j=1}^P \prod_{m=1}^{N_S} \int D\mathbf{r}_i^\alpha(n) D\mathbf{r}_{ij}^\alpha(s) \right. \\ \left. \times D\mathbf{r}_m^\alpha P_0[\mathbf{r}_i^\alpha(n)] P_0[\mathbf{r}_{ij}^\alpha(s)] \delta[\mathbf{r}_{ij}^\alpha(0) - \mathbf{r}^\alpha(\tau_{ij})] \right\rangle. \quad (\text{A6})$$

We now use a mean field theory³⁰ to calculate $\langle R^\sigma \rangle$, i.e., we evaluate the pertinent functional integrals using the saddle-point approximation to obtain the effective free energy. The quenched average over the disordered sequence is also calculated during the process.

First, we introduce the identity

$$1 = \prod_{\alpha=1}^\sigma \int D\boldsymbol{\rho}^\alpha(\mathbf{r}) \delta \left[\rho_A^\alpha(\mathbf{r}) - \sum_{i=1}^{N_C} \int dn \delta[\mathbf{r} - \mathbf{r}_i^\alpha(n)] \right] \\ \times \delta \left[\rho_B^\alpha(\mathbf{r}) - \sum_{i=1}^{N_C} \sum_{j=1}^P \int ds \delta[\mathbf{r} - \mathbf{r}_{ij}^\alpha(s)] \right] \\ \times \delta \left[\rho_S^\alpha(\mathbf{r}) - \sum_{m=1}^{N_S} \delta[\mathbf{r} - \mathbf{r}_m^\alpha] \right] \\ = \prod_{\alpha=1}^\sigma \int D\boldsymbol{\rho}^\alpha(\mathbf{r}) D\boldsymbol{\gamma}^\alpha(\mathbf{r}) \exp \left\{ i \int d\mathbf{r} [\boldsymbol{\gamma}^\alpha(\mathbf{r}) \cdot \boldsymbol{\rho}^\alpha(\mathbf{r})] \right. \\ \left. - i \left[\sum_{i=1}^{N_C} \int dn \gamma_A^\alpha(\mathbf{r}_i^\alpha(n)) \right. \right. \\ \left. \left. + \sum_{i=1}^{N_C} \sum_{j=1}^P \int ds \gamma_B^\alpha(\mathbf{r}_{ij}^\alpha(s)) + \sum_{m=1}^{N_S} \gamma_S^\alpha(\mathbf{r}_m^\alpha) \right] \right\}. \quad (\text{A7})$$

Here $\boldsymbol{\gamma}^T = (\gamma_A, \gamma_B, \gamma_S)$ are fields conjugated to $\boldsymbol{\rho}^T = (\rho_A, \rho_B, \rho_S)$. Substituting the above identity into Eq. (A6) obtains

$$\langle R^\sigma \rangle = \prod_{\alpha=1}^\sigma \int D\boldsymbol{\rho}^\alpha(\mathbf{r}) D\boldsymbol{\gamma}^\alpha(\mathbf{r}) \exp \left\{ i \int d\mathbf{r} \boldsymbol{\gamma}^\alpha(\mathbf{r}) \cdot \boldsymbol{\rho}^\alpha(\mathbf{r}) \right\} \\ \times \left\langle \prod_{i=1}^{N_C} \prod_{j=1}^P \prod_{m=1}^{N_S} \int D\mathbf{r}_i^\alpha(n) D\mathbf{r}_{ij}^\alpha(s) D\mathbf{r}_m^\alpha P[\mathbf{r}_i^\alpha(n)] \right. \\ \left. \times P[\mathbf{r}_{ij}^\alpha(s)] \exp \{ -i \gamma_S^\alpha(\mathbf{r}_m^\alpha) \} \delta[\mathbf{r}_{ij}^\alpha(0) - \mathbf{r}^\alpha(\tau_{ij})] \right\rangle, \quad (\text{A8})$$

where

$$P[\mathbf{r}_i^\alpha(n)] = P_0[\mathbf{r}_i^\alpha(n)] \exp \left\{ -i \int dn \gamma_A^\alpha(\mathbf{r}_i^\alpha(n)) \right\}, \quad (\text{A9})$$

$$P[\mathbf{r}_{ij}^\alpha(s)] = P_0[\mathbf{r}_{ij}^\alpha(s)] \exp \left\{ -i \int ds \gamma_B^\alpha(\mathbf{r}_{ij}^\alpha(s)) \right\}.$$

The part which has to be averaged over the quenched distribution of branch points is

$$\langle Q^\sigma \rangle = \left\langle \prod_{\alpha=1}^\sigma \prod_{i=1}^{N_C} \prod_{j=1}^P \prod_{m=1}^{N_S} \int D\mathbf{r}_i^\alpha(n) D\mathbf{r}_{ij}^\alpha(s) \right. \\ \left. \times D\mathbf{r}_m^\alpha P[\mathbf{r}_i^\alpha(n)] P[\mathbf{r}_{ij}^\alpha(s)] \right. \\ \left. \times \exp \{ -i \gamma_S^\alpha(\mathbf{r}_m^\alpha) \} \delta[\mathbf{r}_{ij}^\alpha(0) - \mathbf{r}^\alpha(\tau_{ij})] \right\rangle \\ = \left\langle \left\{ \prod_{i=1}^{N_C} \prod_{j=1}^P \prod_{m=1}^{N_S} \int D\mathbf{r}_i(n) D\mathbf{r}_{ij}(s) \right. \right. \\ \left. \left. \times D\mathbf{r}_m P[\mathbf{r}_i(n)] P[\mathbf{r}_{ij}(s)] \right. \right. \\ \left. \left. \times \exp \{ -i \gamma_S(\mathbf{r}_m) \} \delta[\mathbf{r}_{ij}(0) - \mathbf{r}(\tau_{ij})] \right\}^\sigma \right\rangle. \quad (\text{A10})$$

We now use a perturbation method and expand $\langle Q \rangle$ in cumulants by powers of the conjugated fields γ_A , γ_B , and γ_S ,

$$Q = Q_0 + Q_1 + Q_2 + Q_3 + Q_4 + \dots, \quad (\text{A11})$$

where Q_n is to the n th power of the conjugated fields. Q_0 is the unperturbed case, and it is easy to obtain $Q_0 = V^{N_C + N_S}$. The linear term Q_1 is zero because of conservation of the total number of molecules of each species. The first non-trivial term is Q_2 . After transforming the fields and propagators into Fourier space, we obtain

$$Q_2 = - \frac{V^{N_C + N_S - 1}}{2} \int d\mathbf{q} \boldsymbol{\gamma}^T(\mathbf{q}) M(\mathbf{q}) \boldsymbol{\gamma}(\mathbf{q}), \quad (\text{A12})$$

where $\boldsymbol{\gamma}^T = (\gamma_A, \gamma_B, \gamma_S)$ and M is a 3×3 matrix,

$$\begin{aligned}
M_{11} &= N_c N^2 g_2 \left(\frac{Nq^2 b^2}{6} \right), \\
M_{22} &= N_c \left[P M^2 g_2 \left(\frac{Mq^2 b^2}{6} \right) \right. \\
&\quad \left. + P(P-1) M^2 g_1 \left(\frac{Mq^2 b^2}{6} \right)^2 g_2 \left(\frac{Nq^2 b^2}{6} \right) \right], \\
M_{12} &= M_{21} = N_c N P M g_1 \left(\frac{Mq^2 b^2}{6} \right) g_2 \left(\frac{Nq^2 b^2}{6} \right), \\
M_{13} &= M_{31} = M_{23} = M_{32} = 0, \\
M_{33} &= N_s,
\end{aligned} \tag{A13}$$

here $g_1(y) = [1 - \exp(-y)]/y$ and $g_2(y) = (2/y^2)[y + \exp(-y) - 1]$. $g_2(y)$ is the so-called Debye function.

From this, we obtain the expression of $\langle Q^\sigma \rangle$,

$$\begin{aligned}
&\left\langle \left(\frac{Q}{V^{N_c + N_s}} \right)^\sigma \right\rangle \\
&= 1 + \frac{1}{V} \sum_{\alpha=1}^{\sigma} \left\{ -\frac{1}{2} \int d\mathbf{q}^\alpha \boldsymbol{\gamma}^T(\mathbf{q}^\alpha) M(\mathbf{q}^\alpha) \boldsymbol{\gamma}(\mathbf{q}^\alpha) \right\} + \dots
\end{aligned} \tag{A14}$$

Now we have

$$\begin{aligned}
\langle R^\alpha[\boldsymbol{\rho}, \boldsymbol{\gamma}] \rangle &= \Pi_{\alpha=1}^{\sigma} \int D\rho^\alpha(\mathbf{q}) D\boldsymbol{\gamma}^\alpha(\mathbf{q}) \exp \left\{ i \int d\mathbf{q} \boldsymbol{\gamma}^\alpha(\mathbf{q}) \right. \\
&\quad \left. \cdot \boldsymbol{\rho}^\alpha(-\mathbf{q}) \right\} \langle Q^\alpha[\boldsymbol{\gamma}] \rangle.
\end{aligned} \tag{A15}$$

As in the case for systems with ordered architectures (e.g., DCPs and triblock copolymers), it is impossible to obtain an analytical formula for the free energy functional by explicitly performing the functional integrations in Eq. (A15). Thus we evaluate these functional integrals using the saddle point approximation. This yields

$$\begin{aligned}
\langle R^\alpha \rangle &[\rho_A, \rho_B, \rho_S, \gamma_A, \gamma_B, \gamma_S] \\
&\approx \langle R^\sigma \rangle_{s.p.} [\rho_A, \rho_B, \rho_S, \gamma_{A_s.p.}, \gamma_{B_s.p.}, \gamma_{S_s.p.}],
\end{aligned} \tag{A16}$$

where $\gamma_{A_s.p.}^\alpha(\mathbf{q})$, $\gamma_{B_s.p.}^\alpha(\mathbf{q})$, and $\gamma_{S_s.p.}^\alpha(\mathbf{q})$ satisfy

$$\begin{aligned}
\frac{\delta \ln \langle R^\sigma \rangle [\rho_A, \rho_B, \rho_S, \gamma_A, \gamma_B, \gamma_S]}{\delta \gamma_A^\alpha(-\mathbf{q})} &= 0, \\
\frac{\delta \ln \langle R^\sigma \rangle [\rho_A, \rho_B, \rho_S, \gamma_A, \gamma_B, \gamma_S]}{\delta \gamma_B^\alpha(-\mathbf{q})} &= 0, \\
\frac{\delta \ln \langle R^\sigma \rangle [\rho_A, \rho_B, \rho_S, \gamma_A, \gamma_B, \gamma_S]}{\delta \gamma_S^\alpha(-\mathbf{q})} &= 0.
\end{aligned} \tag{17}$$

Solving the above equations by iteration, we obtain $\langle S[\boldsymbol{\rho}] \rangle = \lim_{\sigma \rightarrow 0} [\langle R^\sigma \rangle_{s.p.}[\boldsymbol{\rho}] - 1]/\sigma$ as a functional of ρ_A , ρ_B , and ρ_S ,

$$\langle S[\boldsymbol{\rho}] \rangle = -\frac{V}{2} \int d\mathbf{q} \boldsymbol{\rho}^T M^{-1} \boldsymbol{\rho}. \tag{A18}$$

Combining this entropy term with the energy term, we obtain, up to quadratic order, the free energy functional of RGCs in solution,

$$\langle F[\boldsymbol{\rho}] \rangle = \frac{V}{2} \int d\mathbf{q} \boldsymbol{\rho}^T (M^{-1} - D) \boldsymbol{\rho}, \tag{A19}$$

where $D_{ij} = \chi_{ij}$ with i, j being components of type A, B or S.

¹R. Zana, *Surfactant Solutions* (Marcel Dekker, New York, 1987); D. D. Lasic, *Liposomes: From Physics to Applications* (Elsevier, Amsterdam, 1993); R. G. Larson, *The Structure and Rheology of Complex Fluids* (Oxford, New York, 1999); G. Gompper and M. Schick, *Self-Assembling Amphiphilic Systems* (Academic San Diego, 1994); S. A. Safran and N. A. Clark, *Physics of Complex and Supramolecular Fluids* (Wiley, New York, 1987).

²B. M. Discher, Y. Y. Won, D. S. Ege, J. C. M. Lee, F. S. Bates, D. E. Discher, and D. A. Hammer, *Science* **284**, 1143 (1999); Y. Y. Yon, H. T. Davis, and F. S. Bates, *ibid.* **283**, 960 (1999); D. Zhao, J. Feng, Q. Huo, N. Melosh, G. H. Fredrickson, B. F. Chmelka, and G. D. Stucky, *ibid.* **279**, 548 (1998).

³K. P. Johnston, K. L. Harrison, M. J. Clarke, S. M. Howdle, M. P. Heitz, F. V. Bright, C. R. Clarier, and T. W. Randolph, *Science* **271**, 624 (1996); J. M. DeSimone, E. E. Maury, Y. Z. Menceloglu, J. B. McClain, and T. Romack, *ibid.* **265**, 356 (1994).

⁴N. P. Balsara, *Curr. Opin. Solid State Mater. Sci.* **3**, 589 (1998).

⁵S. Karaborni and B. Smit, *Curr. Opin. Colloid Interface Sci.* **1**, 411 (1996); S. Karaborni, K. Esselink, P. A. J. Hilbers, B. Smit, J. Karth'ausser, N. M. van Os, and R. Zana, *Science* **266**, 254 (1994).

⁶R. Lewis, R. N. McElhaney, P. E. Harper, D. C. Turner, and S. M. Gruner, *Biophys. J.* **66**, 1088 (1994); K. Gawrisch, V. A. Parsegian, D. A. Hajduk, M. W. Tate, S. M. Gruner, N. L. Fuller, and R. P. Rand, *Biochemistry* **31**, 2856 (1992); M. W. Tate, E. F. Eikenberry, D. C. Turner, and E. Shyamsunder, *Chem. Phys. Lipids* **57**, 147 (1991).

⁷D. J. Pochan, S. G. Gido, S. Pispas, and J. W. Mays, *Macromolecules* **29**, 5099 (1996).

⁸D. Danino, Y. Talmon, H. Levy, G. Beinert, and R. Zana, *Science* **269**, 1420 (1995); R. Zana, *Curr. Opin. Colloid Interface Sci.* **1**, 556 (1996).

⁹B. Alberts, D. Bray, J. Lewis, M. Raff, K. Roberts, and J. D. Watson, *Molecular Biology of the Cell* (Garland, New York, 1994).

¹⁰M. Xenidou and N. Hadjichristidis, *Macromolecules* **31**, 5690 (1998).

¹¹J. Q. Zhao, E. M. Pearce, T. K. Kwei, J. S. Jeon, P. K. Kesani, and N. P. Balsara, *Macromolecules* **28**, 1972 (1995).

¹²S. Provencher, *Makromol. Chem.* **180**, 201 (1979). In Eq. (1), a and B are instrument related constants.

¹³M. Shibayama, T. Hashimoto, and H. Kawai, *Macromolecules* **16**, 1434 (1983).

¹⁴T. Jian, S. H. Anastasiadis, A. N. Semenov, G. Fytas, G. Fleischer, and A. D. Vilesov, *Macromolecules* **28**, 2439 (1995).

¹⁵The Flory-Huggins (Ref. 16) interaction parameter (χ) for toluene-polystyrene interactions is estimated at 0.43, compared to 0.40, the χ parameter for toluene-polyisoprene interactions. These interaction parameters were measured from subtle small angle neutron scattering measurements on homogeneous and deuterated toluene solutions of polystyrene-polyisoprene block copolymers where the amount of solvent partitioning to the polystyrene-polyisoprene interface was measured (Ref. 17). We are unaware of any direct measurements of this kind for polystyrene-polybutadiene block copolymers. However, given the similarity of the chemical structures of polybutadiene and polyisoprene, and the fact that many materials exhibit similar interactions with polybutadiene and polyisoprene, we conclude that toluene is a slightly selective solvent for the backbone of our branched copolymers.

¹⁶M. L. Huggins, *J. Phys. Chem.* **46**, 151 (1942); P. J. Flory, *J. Chem. Phys.* **10**, 51 (1942).

¹⁷C. I. Huang, B. R. Chapman, T. P. Lodge, and N. P. Balsara, *Macromolecules* **31**, 9384 (1998).

¹⁸Extensive studies of toluene solutions of polystyrene-polyisoprene diblock copolymers with molecular weights as high as 20 000 kg/mol have been conducted and no evidence of micelle formation has been reported (Ref. 19). Studies of toluene solutions of polystyrene-polybutadiene diblock copolymers are not as extensive (Refs. 13, 14)—restricted to molecular weights of 70 kg/mol; but, again, no evidence of micelle formation has been reported.

- ¹⁹A. N. Semenov, S. H. Anastasiadis, N. Boudenne, G. Fytas, M. Xenidou, and N. Hadjichristidis, *Macromolecules* **30**, 6280 (1997).
- ²⁰L. Leibler, H. Orland, and J. C. Wheeler, *J. Chem. Phys.* **79**, 3550 (1980).
- ²¹S. Qi, A. K. Chakraborty, H. Wang, A. A. Lefebvre, and N. P. Balsara, *Phys. Rev. Lett.* **82**, 2896 (1999).
- ²²S. Qi, A. K. Chakraborty, and N. P. Balsara, *J. Chem. Phys.* (in press).
- ²³S. F. Edwards and P. W. Anderson, *J. Phys. F* **5**, 965 (1975).
- ²⁴A. Shinozaki, D. Jasnow, and A. C. Balazs, *Macromolecules* **27**, 2496 (1994).
- ²⁵S. Qi and A. K. Chakraborty, *J. Chem. Phys.* (in press).
- ²⁶We have used the simplest model that captures the essential physics of the problem, and hence we consider the backbone segments to be chemically identical to the solvent molecules. In this respect, it is similar in spirit to that of Leibler *et al.* for diblock copolymer micelles (Ref. 19). In the model, the grafting points are located at one end of the branch while in the experiments, the grafting points are located at the middle of the branch. These simplifications do not affect the qualitative trends that we predict.
- ²⁷P. D. Olmsted and S. T. Milner, *Phys. Rev. Lett.* **72**, 936 (1994).
- ²⁸D. G. Walton, P. P. Soo, A. M. Mayes, S. J. Sofia Allgor, J. T. Fujii, L. G. Griffith, J. F. Anker, H. Kaiser, J. Johansson, G. D. Smith, J. G. Barker, and S. K. Satija, *Macromolecules* **30**, 6974 (1997).
- ²⁹M. R. Anklam, D. A. Saville, and R. K. Prud'homme, *Langmuir* **15**, 7299 (1999).
- ³⁰K. M. Hong and J. Noolandi, *Macromolecules* **14**, 727 (1981).